

DETAILED MECHANICS OF MEMBRANE-MEMBRANE ADHESION AND SEPARATION

II. Discrete Kinetically Trapped Molecular Cross-Bridges

EVAN A. EVANS

*Department of Pathology, University of British Columbia, Vancouver, British Columbia, Canada
V6T 1W5*

ABSTRACT In general, membrane-membrane adhesion involves specific molecular binding and cross-bridging reactions. The ideal, classical view is that near equilibrium the forces required to separate adhesive contacts are essentially equal to those induced in the membrane when the contact is formed. In contrast to the classical view, experimental observations often show that negligible levels of tension are induced by the adhesive contact even though the tension required to separate the contact is large enough to rupture the membrane. The deviation in tension levels associated with contact formation and separation appears to be due to the sparse distribution of strong molecular cross-bridges. Here, the mechanics of membrane-membrane adhesion and separation is developed for the case of discrete, kinetically trapped cross-bridges. The solution is obtained by numerical computation of the membrane contour that minimizes the total free energy (membrane elastic energy of deformation plus cross-bridge energies) in the contact zone. This solution is matched with the analytical solution for membrane stresses and geometry derived for the adjacent, unbridged zone. The results yield specific values of the macroscopic tension applied to the membrane in the plane region away from the contact zone and the microscopic angle at the edge of the contact zone. Two disparate values of the macroscopic tension are found: (a) the minimum tension required to separate the adherent membranes; and (b) the maximum tension induced in the membranes when the contact is formed (i.e., the level of tension at which the contact will just begin to spread). The results show that the deviation between these two tensions can be very large and depends strongly on the surface density of cross-bridges. In addition, the results provide an estimate of the restraining forces that anchor receptors within the plane of the membrane.

INTRODUCTION

In the preceding paper (1), the mechanics of membrane-membrane adhesion were examined for the case where the adhesive cross-bridging forces between the membranes are distributed continuously over the surfaces but with a finite extent of interaction away from each surface. For the continuum model, the tension necessary to oppose spreading of a membrane-membrane contact is equal to the minimum level of tension required to separate adherent membranes. Also, the macroscopic tension applied to the membrane in the free region away from the contact is given by the classical Young equation, which relates the free energy reduction per unit area for formation of planar contact to the membrane tension and macroscopic contact angle. The continuum model has been shown to be a valid representation for adhesion and separation of synthetic, phospholipid bilayer membrane vesicles that were allowed to aggregate either via van der Waal's attraction (2) or in high molecular weight glucose polymer (dextran) solutions (3). It also appears to be an appropriate model for red cell rouleaux formation (4, 5).

In contrast with these observations of uniform spreading and the equality of membrane tensions that result from spreading and that are necessary to separate adhesive contact, experiments often show that there is little or no tendency for membrane-membrane contact to spread (i.e., a negligible level of tension is induced by the formation of the contact) even though the tension required to subsequently separate the contact is very large (6). The deviation of the level of tension induced in the membranes by contact formation from that required to separate the contact appears to be due to the sparse distribution of strong molecular cross-bridges. Thus, the purpose of this paper is to consider the mechanics of membrane-membrane adhesion and separation for discrete molecular cross-bridges.

The cross-bridging sites (receptors) in membranes are not stationary but are, to some extent, mobile in the plane of the membrane. Here it will be assumed that the receptors are kinetically trapped (i.e., stationary). This assumption is equivalent to the statement that the surface diffusion of receptors is much slower than the reactions for formation and breakage of cross-bridges. Experimentally,

this assumption would be consistent with rapid formation (spreading) of membrane-membrane contact to a nearly static, equilibrium configuration (no apparent time variation). The rapid spreading would be limited only by viscous dissipation in the membrane and adjacent media, not by reaction kinetics or receptor diffusion. Similar, rapid deformation followed by static configurations are observed when red cells adhere via dextran polymer, lectin, or antibody cross-bridges (4, 6). If, on the other hand, the receptors were highly mobile, it is expected that there would be an accumulation of cross-bridges with time and perhaps a gradual increase in the size of the contact zone. This appears to be the situation for macrophages left to spread for fractions of an hour or more on substrates coated with immobilized immune complexes (7). A model for the situation of total kinetic freedom for receptors has been proposed (8, 11); in the Appendix of the first paper (1), it was shown how the approach of these authors could be expanded to include mechanical equilibrium and time-dependent contact formation. Currently, models do not represent active (driven) processes of adhesion and engulfment (e.g., phagocytosis). However, for the initial phase of surface recognition and adhesion, it is expected that the model of kinetically trapped receptors is a reasonable approximation. Subsequent slow diffusion (accumulation) of receptors can be considered simply as a sequence of static distributions of cross-bridges.

Another reason for the detailed analysis of membrane stresses proximal to and within the adherent zone is to evaluate the lateral forces that act to drag cross-bridges and accumulate them at the edge of the contact zone when membranes are separated. This effect has been observed when red blood cells that have been bound together by plant lectins are separated (6). With the calculation of lateral forces that act on cross-bridges and measurements of cross-bridge accumulation at the edge of the contact zone (e.g., by fluorescence microscopy), estimates can be made of the restraining forces that anchor receptors within the plane of the membrane.

The approach here is to determine the equilibrium geometry of a membrane-membrane contact held together by discrete cross-bridges; the solution is obtained by numerical computation of the membrane contour that minimizes the total free energy (membrane elastic energy of deformation plus cross-bridge energies) in the contact zone. This solution is then matched with the analytical solution for membrane stresses and geometry that was obtained previously for the adjacent, unbridged zone (1). The results yield specific values of the macroscopic tension applied to the membrane in the plane region away from the

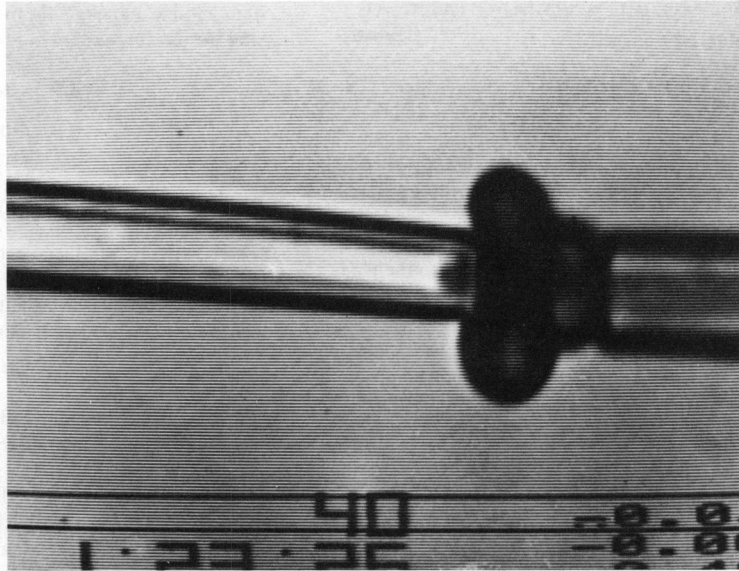
contact zone (normalized by the work or free energy of cross-bridge formation per unit area) and the microscopic contact angle at the edge of the contact zone. Two disparate values of the macroscopic tension are found: (a) the level of tension that stresses the first cross-bridge at the edge of the contact zone to the near breaking point; and (b) the reduced level of tension that will just permit the membranes to approach sufficiently for the next cross-bridge to form adjacent to the contact zone. The former is the minimum tension required to separate adherent membranes; the latter is the maximum tension induced in the membranes when contact is formed (i.e., the level of tension at which the contact will just begin to spread). Deviation from either of these two tensions can be very large and will be shown to depend strongly on the surface density of cross-bridges, consistent with experimental observations.

EXAMPLE OF ADHESION/SEPARATION BEHAVIOR FOR DISCRETE CROSS-BRIDGES

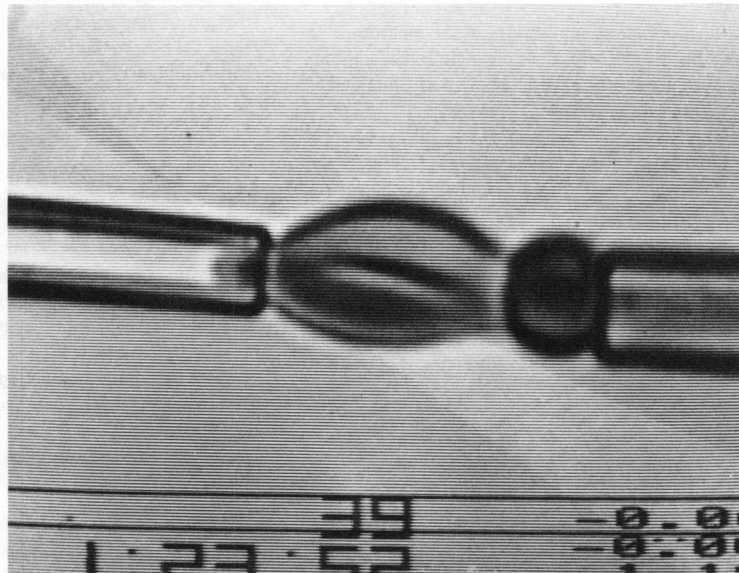
In contrast to the adhesion/separation behavior expected for continuous adhesive forces between membranes, membrane-membrane adhesion via a sparse distribution of cross-bridges is characterized by little or no tendency to spread when the membrane capsules are brought into contact and by the requirement for large membrane tensions in order to separate the contact after formation. An example of this behavior is shown in Fig. 1 where two red blood cells have been maneuvered into proximity to test adhesion (6). The cell on the left was first equilibrated with a solution that contained the plant lectin wheat germ agglutinin (WGA) at $\sim 10^{-7}$ M concentration; this cell was aspirated by a high suction pressure so that it formed a rigid, spherical test surface outside the pipette and was transferred to a second chamber, which contained red cells in WGA-free buffer. A second red cell was aspirated with low suction pressure so that it remained a flaccid discocyte and then was positioned just to contact the WGA-coated test cell. No spontaneous spreading of the flaccid cell surface on the test cell was observed even though adhesive contact had been formed. (By comparison, if a high molecular weight polymer like dextran was in the solution at the proper concentration [9], rapid spreading and encapsulation of the test surface always occurred.) Based on the measured values of red cell membrane elastic moduli, the threshold free energy reduction per unit area that is sufficient to initiate spreading is calculated to be $\sim 5-10 \times 10^{-4}$ erg/cm; appropriate to this threshold level, tension levels of 10^{-3} dyn/cm would be induced in the red cell membrane (10). Subsequent separation of the WGA-adherent red cells required large suction pressures and caused significant elastic deformation of the flaccid cell as shown in Fig. 1. Values of the tension near the contact zone were calculated to be from 0.1–1 dyn/cm over the range of equilibrium separation steps (6). Clearly, there was an enormous difference between the negligible tension associated with contact formation and the large tensions required to separate the contact. Similar behavior has been observed with other lectins and monoclonal antibodies to red cell surface glycoproteins. For all of these situations, the number of receptors on the red cell surface is estimated to be $\sim 10^6$ or equivalent to $10^{12}/\text{cm}^2$ (i.e., 100 \AA^2 per molecule).

FIGURE 1 Videomicrographs of the step-wise separation of red blood cells that have adhered via WGA cross-bridges. The cell on the right was first coated with WGA, aspirated into a rigid spherical surface, and transferred to the chamber that contained only red blood cells in WGA-free buffer. The cell on the left (uncoated) was then maneuvered into position and adhesive contact was made as shown in the top panel. The flaccid cell on the left was subsequently separated in steps at which the force of attachment was measured from the pipette suction pressure and cell geometry as shown in the lower panels. (Take from Evans and Leung, 1984).

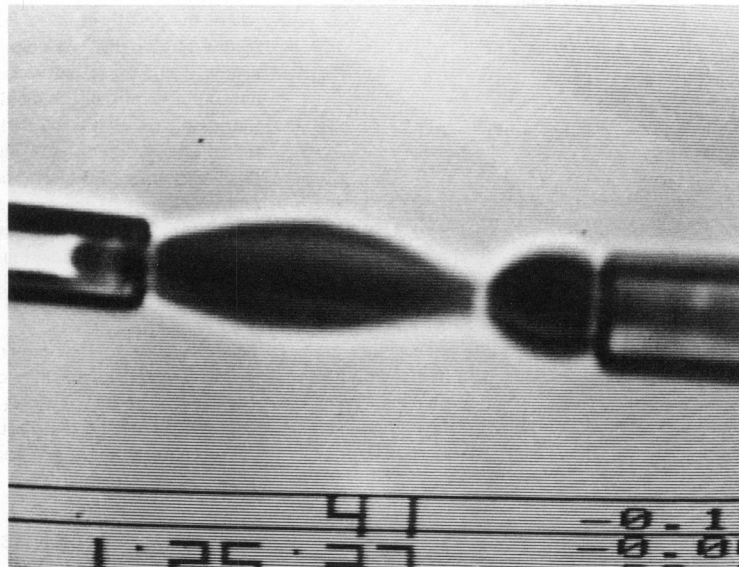
a



b



c



ADHESION MODEL AND MECHANICAL EQUILIBRIUM

As in the previous development for continuous cross-bridges (1), the analysis here considers the cross-bridging (adhesion) forces as finite range interactions. Thus, at equilibrium, there are two membrane regions: (a) a free (unbridged) zone where the membranes are not subject to attractive forces; and (b) an adherent (bridged) zone where the membranes are held together by attractive cross-bridging forces. This is illustrated in Fig. 2. As before, the membrane is treated as an elastic continuum where the discrete cross-bridging forces are assumed to act normal to the plane of adhesive contact as illustrated in Fig. 2. The approach is to determine the membrane contour that will minimize the total free energy (elastic deformation energy plus cross-bridge energies) in the contact zone and then to require continuity of this solution with the analytical solution determined previously for the free (unbridged) region (1). Because of the high curvature adjacent to the edge of the contact zone, the problem is reduced to consideration of the contour in the meridional plane that depends only on the curvilinear coordinates (s, θ) of the membrane as illustrated in Fig. 2. Also shown in Fig. 2 are the intensive forces (membrane tension, T_m , and transverse shear, Q_m) that are supported by the membrane (10). In the macroscopic region away from the adherent zone, the membrane is subject to a uniform tension, T_m^0 , where the membrane forms a macroscopic (observable) contact angle of θ_0 with respect to the other surface.

Recalling the solution for mechanical equilibrium of the membrane in the free (unbridged) region, the distribution of membrane tension, transverse shear, and membrane curvature were obtained as functions of

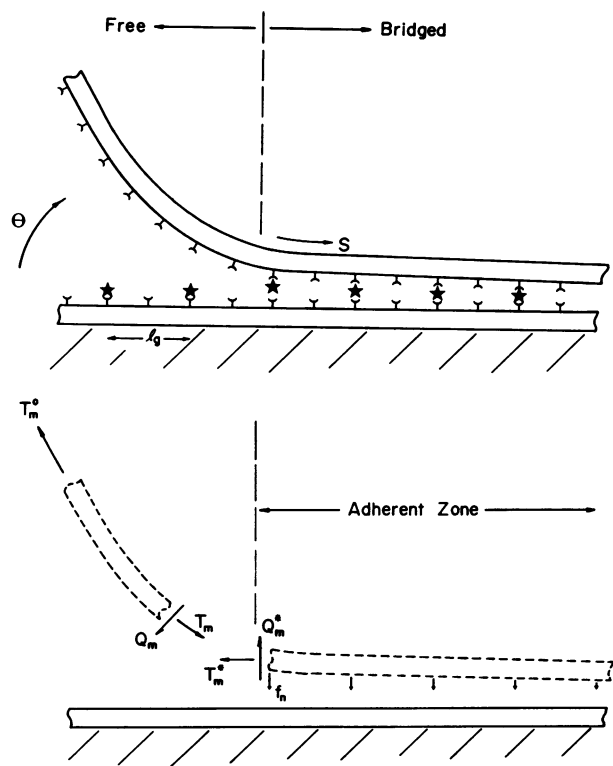


FIGURE 2 Schematic illustration of the adherent (bridged) and free (unbridged) zones proximal to the edge of the contact zone. The discrete forces that arise from cross-bridges between membrane receptors are illustrated as well as the intensive forces supported by the membrane surface itself. In addition to the attractive forces, f_n , the membrane supports a principal tension, T_m , which acts tangent to the plane of the membrane, and a transverse shear, Q_m , which acts normal to the membrane surface.

the curvilinear angle, θ , the macroscopic tension applied to the membrane, and the membrane curvature elastic or bending modulus, B .

$$\begin{aligned} T_m &= T_m^0 \cdot \cos(\theta_0 - \theta) \\ Q_m &= T_m^0 \cdot \sin(\theta_0 - \theta) \\ (K_m)^2 &= \left(\frac{2 \cdot T_m^0}{B} \right) [1 - \cos(\theta_0 - \theta)] + (K_m^0)^2. \end{aligned} \quad (1)$$

These variables are made continuous with the solution obtained for the adherent (bridged) zone.

In the adherent zone, the total free energy functional includes membrane elastic deformation plus cross-bridge energies,

$$F = F_{ED} + F_{CB}. \quad (2)$$

This functional is minimized in conjunction with the work required to displace forces at the boundaries; the variation is taken with respect to the parameters that characterize the membrane contour in the contact zone. The same approximation to the intermolecular force, f_n , will be employed here as used previously for the continuous cross-bridge model (1). The approximation considers that the force-displacement relation for the cross-bridges is linear up to a maximum (breaking) force and that there is zero restoring force for greater bond extensions.¹ The displacement of the bond from equilibrium is represented by the variable ζ with the maximum strength of the bond given by \hat{f}_n at an extension or bond length of ℓ_b . Hence, the contribution to the total free energy from extension of the cross-bridges is given by the approximation,

$$F_{CB} = \frac{1}{2} (\hat{f}_n \cdot \ell_b) \sum_{i=0}^N \zeta_i^2, \quad (3)$$

where N is the number of cross-bridges involved in the adhesive contact and the product, $F_b = \hat{f}_n \cdot \ell_b/2$, is the free energy change (work) which results from formation (-) or breakage (+) of a single cross-bridge. The initial value for the sum of cross-bridge energies ($i = 1$ or 2) is determined by one of two situations: (a) $i = 1$ when a cross-bridge is maximally stretched at the edge of the contact zone; this is the case for separation of the adherent contact. (b) $i = 2$ when a cross-bridge is about to be formed at the edge of the contact (given by the lattice position $i = 1$) but no attractive force is present. This is the condition for minimal spreading of the contact.

The free energy functional for elastic deformation of the membrane is given by (10),

$$\begin{aligned} F_{ED} &= \left(\frac{B \cdot \ell_g}{2} \right) \int_0^{N \cdot \ell_g} (K_m - K_m^0)^2 ds \\ &\quad + \ell_g \cdot \int_0^{N \cdot \ell_g} (T_m \cdot \epsilon) ds, \end{aligned} \quad (4)$$

where the first term is the bending or curvature elastic energy and the second term is the work for in-plane extension of the membrane. The principal curvature of the contour is K_m ; K_m^0 is the unstressed or the natural curvature of the membrane, which will be assumed to be zero in the sample calculations; ϵ is the measure of strain along the contour (i.e., the fractional extension of membrane elements). The free energy equations for membrane deformation and cross-bridge extension, Eqs. 3 and 4, represent the total energy of a strip of membrane that has a width of ℓ_g . The parameter ℓ_g is the average distance between cross-bridge sites and thus represents the dimension of a lattice on the surface.² In the region of

¹See Appendix of first paper (1) for discussion of the physical force approach in relation to chemical equilibrium.

²The parameter ℓ_g represents the regional grouping of receptors for a nonuniform (patchy) distribution on the cell surface. It is assumed that the receptor patches are spaced, on the average, by ℓ_g separation distance.

high curvature that characterizes the membrane contour close to and within the adherent zone, membrane bending energy determines the shape of the contour so the in-plane (extensional) elasticity will be neglected. As such, the membrane tension acts as a Lagrange multiplier in Eq. 4 with the auxiliary requirement that the local strain approach zero, i.e.,

$$\epsilon \rightarrow 0. \quad (5)$$

This means that each membrane segment between cross-bridge sites is inextensible. The result is that the density of cross-bridge sites remains uniform and constant.

Mechanical equilibrium is defined by the expression that the variation in total free energy is equal to the variation in work required to displace forces at the boundaries, which must be satisfied in association with the

$$\delta W_B = \delta F \quad (6)$$

constraint equation, Eq. 5. The virtual work required to displace forces at the boundaries reduces to the virtual displacement of the macroscopic tension T_m^0 supported by the membrane in the planar region away from the contact zone,

$$\delta W_B = T_m^0 \cdot \delta s_0, \quad (7)$$

where δs is the virtual displacement of the membrane in the direction tangent to the surface. Eq. 7 presumes that the membrane contour in the free (unbridged) zone is that prescribed by Eqs. 1 and that the membrane surface is inextensible.

Solution of Eqs. 5, 6, and 7 is obtained by iterative, numerical computation of the membrane contour that minimizes the functional consistent with the constraint requirements and the forces at the boundaries. The contour is defined by displacements (z, r) from initial positions in the membrane; z is the displacement normal to the plane of the adhesive contact; r is the lateral displacement in the plane of the contact. Hence, the cross-bridge extensions are given by,

$$\zeta_i = z_i. \quad (8)$$

The contact angle, θ , and curvature, K_m , of the membrane contour are given by,

$$\theta = \sin^{-1} \left(-\frac{dz}{ds} \right)$$

$$K_m = -\frac{d^2z}{ds^2} / \cos \theta,$$

which, for contact angles $< 30^\circ$, can be well approximated by

$$\theta \approx -\frac{dz}{ds}$$

$$K_m \approx -\frac{d^2z}{ds^2}. \quad (9)$$

The measure of strain, ϵ , along the membrane contour is given by,

$$\epsilon = \frac{dr}{ds} + \frac{1}{2} \left[\left(\frac{dr}{ds} \right)^2 + \left(\frac{dz}{ds} \right)^2 \right].$$

Solutions to the variational expression for mechanical equilibrium are restricted to the class of contours that are locally inextensible; hence this equation reduces to,

$$\frac{dr}{ds} \left[1 + \frac{1}{2} \left(\frac{dr}{ds} \right)^2 \right] = -\frac{1}{2} \left(\frac{dz}{ds} \right)^2,$$

which, for contact angles $\leq 30^\circ$, is well approximated by,

$$\frac{dr}{ds} = -\frac{1}{2} \left(\frac{dz}{ds} \right)^2. \quad (10)$$

The result is that the lateral displacements are determined by the normal displacements and a single function, $z(s)$, completely specifies the contour. For this class of contours, the variational statement of equilibrium reduces to

$$0 = \left(\frac{\hat{f}_n \cdot \ell_b}{B} \right) \sum_{i=0,1}^N z_i \cdot \delta z_i$$

$$+ \ell_g \cdot \int_0^{N \cdot \ell_g} (K_m - K_m^0) \cdot \delta K_m \cdot ds - T_m^0 \cdot \delta s_0. \quad (11)$$

The method of solution utilizes a Newton-Raphson iterative solution to Eq. 11 where the displacement function, $z(s)$, is a piece-wise continuous function with continuous first and second derivatives. The contour functions are called Spline functions (11),

$$z(s) = \sum_{j=0}^3 C_{ij} (s - s_i)^j, \quad s_i \leq s < s_{i+1}. \quad (12)$$

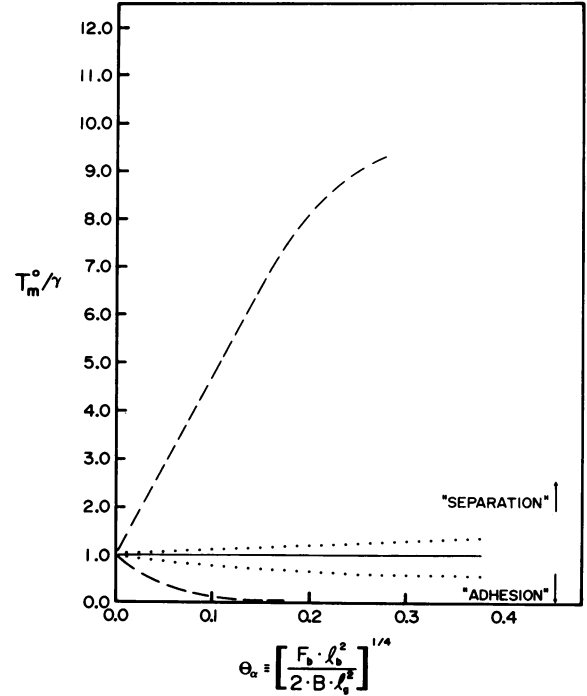


FIGURE 3 The macroscopic tension applied to the membrane in a plane region away from the contact zone, normalized by the adhesion energy per unit area, is plotted vs. the dimensionless parameter that represents the ratio of adhesion to bending (deformation) energies. These results are for the specific case where the macroscopic contact angle (θ_0) is 90° and for two ratios, ℓ_g/ℓ_b , of cross-bridge spacing to bond length, 1:1 (···) and 10:1 (---). For each cross-bridge density (ℓ_g/ℓ_b), two levels of tension are predicted: (a) an upper value which represents the minimum level of tension required to separate the adhesive contact; (b) a lower value that characterizes the maximum level of tension that will just allow the contact to spread. Even for moderately dense cross-bridges ($\ell_g/\ell_b = 1$), the tension for separation deviates from the level of tension which will allow the contact to spread. The solid line (—) is the level of tension predicted from the classical Young equation where there is no deviation between the minimum tension required to separate adhesive contact and the tension that will allow the contact to spread.

The positions, s_i , are the curvilinear locations of cross-bridge sites; the coefficients, C_{θ} , are the displacements normal to the plane of the adherent contact at each cross-bridge site. The solution is required to be continuous with the solution, Eqs. 1, at the intersection with the free unbridged zone.

RESULTS AND DISCUSSION

Solution to the variational expression, Eq. 11, coupled with the continuity requirement at the intersection with the unbridged zone yields specific values of the macroscopic tension for each macroscopic contact angle. In addition, there are two levels of tension predicted for each contact angle: (a) an upper value which represents the minimum level of tension required to separate the adhesive contact; (b) a lower value which characterizes the maximum level of tension that will just allow the contact to spread. The tension values are obtained in dimensionless form, normalized by the work or energy, γ , of cross-bridge separation per unit area of membrane-membrane contact; i.e.,

$$\tilde{T}_m^0 \equiv T_m^0/\gamma,$$

where

$$\gamma \equiv F_b/\ell_g^2 = (\hat{f}_n \cdot \ell_b/2 \cdot \ell_g^2).$$

The ideal, Young equation predicts that the macroscopic tension normalized by the adhesion energy density is only a function of the macroscopic contact angle, θ_0 ,

$$T_m^0/\gamma = 1/(1 - \cos\theta_0).$$

This ideal relation is appropriate for an infinitely dense (continuum) cross-bridge lattice (1) where there is no deviation between the minimum tension required to separate adhesive contact and the maximum tension that will allow the contact to spread. Fig. 3 shows the two levels of dimensionless tension determined for a macroscopic contact angle of 90° plus two ratios, ℓ_g/ℓ_b , of cross-bridge spacing to bond length, 1:1 and 10:1. As shown in Fig. 3, the tension values depend on the dimensionless parameter, θ_α ,

$$\theta_\alpha \equiv (F_b \cdot \ell_b^2/2 \cdot B \cdot \ell_g^2)^{1/4},$$

which represents the ratio of adhesion to bending (deformation) energies. In the previous continuum development (1), the inverse of this parameter represented the spatial width of the boundary layer over which bonds are stretched at the edge of the contact zone. As expected, the two levels of tension approach the ideal value from the Young

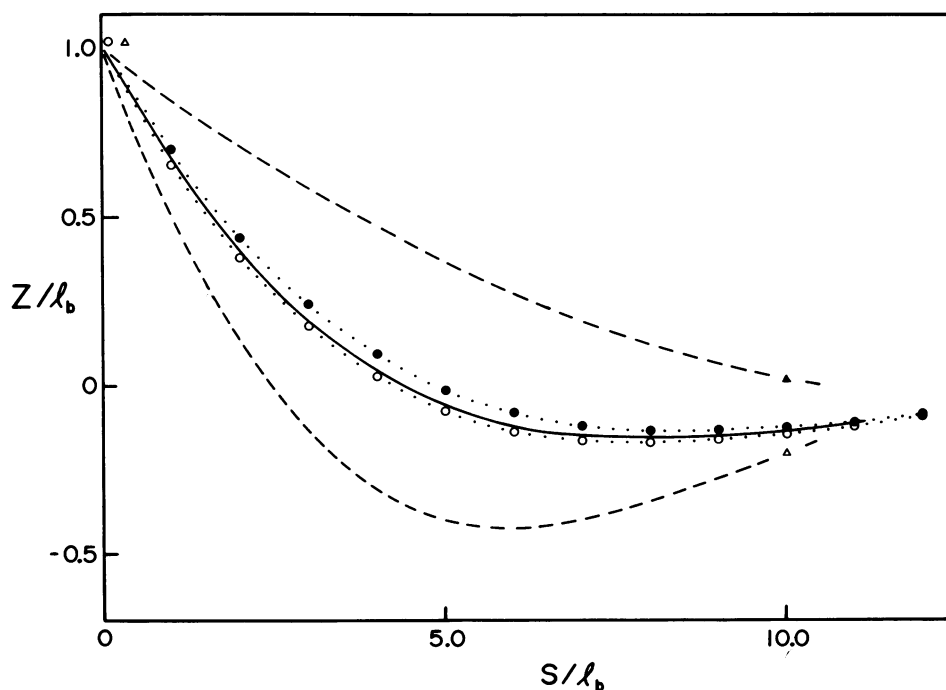


FIGURE 4 Membrane contours are shown for two ratios, ℓ_g/ℓ_b , of cross-bridge spacing to bond length, 1:1 (· · ·) and 10:1 (---), and a specific value of the parameter for adhesion to bending energy ratio θ_α , 0.211, and a macroscopic contact angle (θ_0) of 90° . Open circles and solid circles represent separation and adhesion, respectively ($\ell_g/\ell_b = 1.0$). Open and solid triangles represent separation and adhesion, respectively ($\ell_g/\ell_b = 10.0$). Also shown is the contour (—) derived previously from the continuum model where the cross-bridges were assumed to be infinitely dense (1). For relatively dense populations of cross-bridges, the contours deviate only slightly from that predicted by the continuum model (—). However, for low densities (i.e., $\ell_g/\ell_b = 10$), there is significant deviation of the contours from the continuum solution. Bond sites are represented by Δ , \blacktriangle , \circ , \bullet . Note there are no bonds formed at the first receptor site (i.e., no solid circle and no solid triangle) for the situation where the contact is about to spread to the next site. The displacement axis is greatly enlarged in comparison to the axis for the curvilinear distance along the membrane.

equation when the density of cross-bridge sites becomes large.

There is a specific membrane contour and microscopic contact angle associated with each equilibrium level of tension. Fig. 4 shows the contours in the adherent zone determined for two ratios, l_g/l_b , of cross-bridge spacing to bond length, 1:1 and 10:1, and a specific value of the ratio of adhesion to bending energies. Also shown is the contour derived previously from the continuum model where the cross bridges are assumed to be infinitely dense. (Fig. 5 shows the progressive increase in microscopic contact angle at the edge of the contact zone as the ratio of adhesion to bending energies is increased.) It is apparent that the contours (one for separation and the other for spreading of the contact) and microscopic contact angles deviate only slightly from the continuum solution when the cross-bridges are relatively dense (i.e., $l_g/l_b = 1$), whereas the contours and angles deviate appreciably from the continuum solution when the cross-bridge density is low (i.e., $l_g/l_b = 10$). It is also apparent that when the cross-bridge density is low, only the first cross-bridge is significantly stressed. Also, when the sites are far apart, the tension must be reduced to nearly zero to permit the next cross-bridge to form; thus, there is little or no tendency for the contact to spread unless the surfaces are forced together. Since nearly all of the stress is taken by the first cross-bridge site at the edge of the contact zone when the density is low, the tension required to separate the contact greatly exceeds the value anticipated from the Young equation. The level of tension required to separate the contact approaches the value predicted by the Young equation multiplied by the ratio of the cross-bridge spacing to bond length, when the cross-bridge density is low,

$$T_m^0/\gamma \rightarrow (l_g/l_b)/(1 - \cos \theta_0).$$

This relation shows that the average work required to separate adhesive contact per unit area is equal to the adhesion energy density, γ .

Another interesting feature that results from the analysis is the prediction of the lateral forces applied to each cross-bridge (receptor). Fig. 6 shows the dimensionless lateral force applied to cross-bridges for two levels of density ($l_g/l_b = 1, 10$) and a specific ratio of adhesion to bending energies. For low densities, essentially only the first site is subject to a lateral force, whereas for higher densities the lateral forces are distributed over several cross-bridge sites. The implication is that for low densities, the lateral forces will act to displace and accumulate sites at the edge of the contact zone and as such will essentially form a stiffened line of cross-bridges. As the accumulation proceeds, the tension required to separate the contact will become progressively larger. This effect has been observed previously when adherent red cells were separated (6).

The results clearly show that the density of cross-bridge sites must be determined along with the mechanical stresses associated with membrane-membrane adhesion/

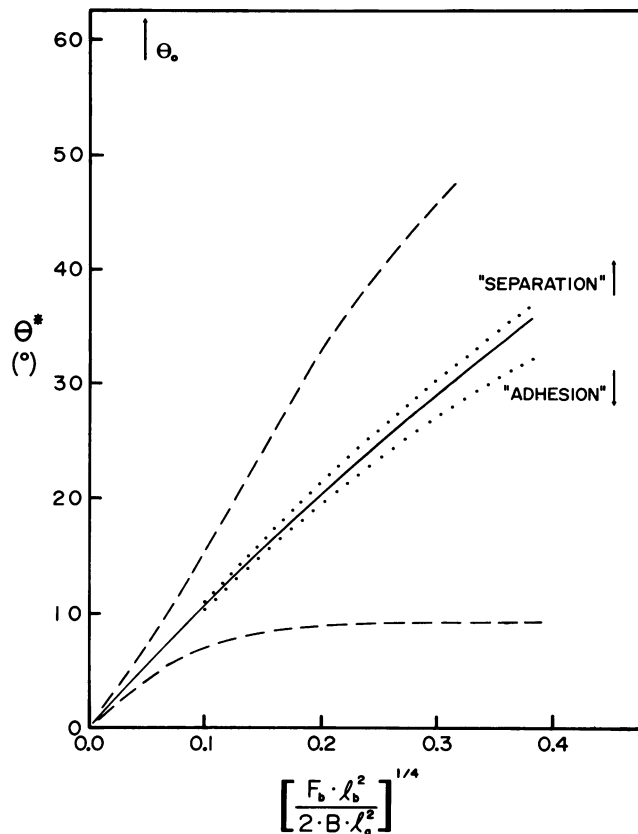


FIGURE 5 Values for the microscopic contact angle at the edge of the contact zone are plotted as a function of the parameter that represents the ratio of adhesion to bending energies for a specific value of the macroscopic contact angle (Θ_0) of 90° . The solid line (—) is the microscopic contact angle derived from the continuum solution where the cross-bridges are assumed to be infinitely dense. There are two broken curves plotted for each ratio, l_g/l_b , of cross-bridge spacing to bond length, 1:1 ($\cdot \cdot \cdot$) and 10:1(---). The upper broken curves represent the situation where the contact is separated and the lower curves are appropriate to the situation where the contact is about to spread.

separation to derive the intrinsic properties of molecular bridging forces and energies. Also, because of the paucity of receptors in biological membrane surfaces, mechanical properties of the substrates will always interfere with the initial recognition and adhesion process. Once contact is established subsequent separation may be very difficult and the contact may be increased by active and passive deformation of the cells themselves. The usefulness of model calculations such as these is that controlled adhesion experiments can be analyzed to provide not only information about molecular forces and energies but also information about the forces that anchor receptors within the membrane.

This work was supported in part by National Institutes of Health grant HL 26965 and Canadian MRC grant MT 7477.

Received for publication 27 June 1984 and in final form 18 January 1985.

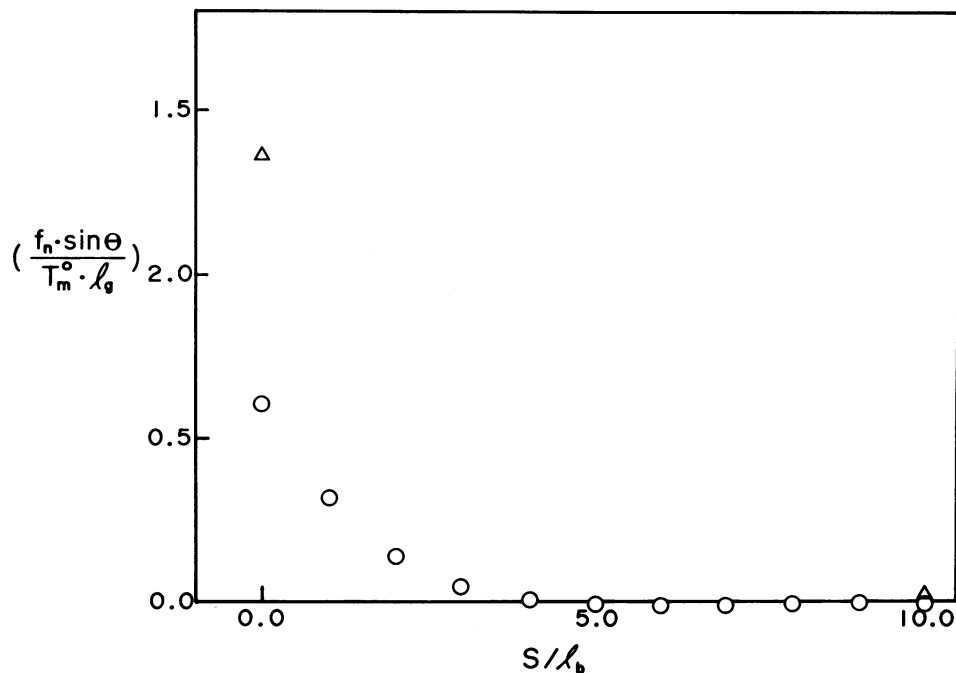


FIGURE 6 The lateral force applied to cross-bridges, normalized by the macroscopic tension times the cross-bridge spacing, is plotted vs. cross-bridge position for a specific value of the parameter for adhesion to bending energy ratio and a macroscopic contact angle (θ_0) of 90° . $\theta_a = 0.211$. The triangles are for a cross-bridge density given by $l_g/l_b = 10$ and the circles are for a cross-bridge density given by $l_g/l_b = 1$. These lateral forces would act to accumulate cross-bridges (receptors) at the edge of the contact zone.

REFERENCES

1. Evans, E. A. 1985. Detailed mechanics of membrane-membrane adhesion and separation: I. Continuum of molecular cross-bridges. *Biophys. J.* 48:175-183.
2. Evans, E. A., and M. Metcalfe. 1984. Free energy potential for aggregation of giant, neutral lipid bilayer vesicles by van der Waal's attraction. *Biophys. J.* 46:423-426.
3. Evans, E. A., and M. Metcalfe. 1984. Free energy potential for aggregation of mixed PC:PS lipid vesicles in glucose polymer (dextran) solutions. *Biophys. J.* 45:715-720.
4. Buxbaum, K., E. A. Evans, and D. E. Brooks. 1982. Quantitation of surface affinities of red blood cells in dextran solutions and plasma. *Biochemistry.* 21:3235-3239.
5. Skalak, R., P. R. Zarda, K.-M. Jan, and S. Chien. 1981. Mechanics of rouleau formation. *Biophys. J.* 35:771-782.
6. Evans, E. A., and A. Leung. 1984. Adhesivity and rigidity of red blood cell membrane in relation to WGA binding. *J. Cell Biol.* 98:1201-1208.
7. Michel, J., M. M. Pieczonka, J. C. Unkeless, G. I. Bell, and S. C. Silverstein. 1983. Fc receptor modulation in mononuclear phagocytes maintained on immobilized immune complexes occurs by diffusion of the receptor molecule. *J. Exp. Med.* 157:2121-2139.
8. Dembo, M., and G. I. Bell. 1984. The thermodynamics of cell adhesion. *In Current Topics in Membranes and Transport Vol. 22*, In press.
9. Evans, E. A. 1980. Minimum energy analysis of membrane deformation applied to pipet aspiration and surface adhesion of red blood cells. *Biophys. J.* 30:365-284.
10. Evans, E. A., and R. Skalak. 1980. *Mechanics and Thermodynamics of Biomembranes*. CRC Press, Inc., Boca Raton, Florida.
11. Bell, G. I., M. Dembo, and Bongrand, P. 1984. Cell-cell adhesion: competition between nonspecific repulsion and specific bonding. *Biophys. J.* 45:1051-1064.